Armstrongite at non ambient conditions: An *in-situ* high temperature single crystal X-ray diffraction study

M. Lacalamita[a, *] (erase the superscript ",*" after the superscript "a")

emanuela.schingaro@uniba.it (erase emanuela.schingaro@uniba.it below M. Lacalamita)

G. Cametti[b]

E. Mesto[c]

E. Schingaro[c] (add the superscript ",*" after the superscript "c") (add emanuela.schingaro@uniba.it below E.Schingaro)

[a]Dipartimento di Scienze della Terra - Università di Pisa, via S. Maria 53, I-56100 Pisa, Italy

[b]Mineralogical Crystallography, Institute of Geological Sciences, University of Bern, Baltzerstrasse 1-3, 3012, Bern, Switzerland

[c]Dipartimento di Scienze della Terra e Geoambientali - Università degli Studi di Bari "Aldo Moro", via E. Orabona 4, I-70125 Bari, Italy

[*]Corresponding author.

Abstract

The dehydration process of armstrongite, $CaZr[Si_6O_{15}]\cdot 2H_2O$, from Khan Bogdo deposit (Gobi, Mongolia) was studied by *in-situ* High Temperature Single Crystal X-ray Diffraction (HT SCXRD) in air from 25 to 500 °C and in N_2 atmosphere from 25 to 375 °C. An abrupt discontinuity in the trend of the *a* and *b* parameters and of the unit-cell volume was observed at T = 275 °C in dry conditions and at T = 450 °C in air. This discontinuity is associated to dehydration and to a first-order transition. When compared to RT armstrongite, the dehydrated phase structure (obtained at 275 °C only under dry conditions) is characterized by the same space group (*C*2/*m*), cell volume decrease of ~7.5%, compatible with the loss of the two water molecules, positional disorder of Ca over three sites, splitting of some of the heteropolyhedral framework oxygen atoms, tilting of Zr octahedra and Si tetrahedra and, distortion of four-, six- and eight-membered channels. Differently from other Zr-silicate structures, the channels dimension of the dehydrated structure (defined as the ratio between the longest and shortest diagonals of the channels) allowed the armstrongite structure to completely recover the structural water after 21 days exposure to humid conditions.

Keywords: Armstrongite; Zeolite-like; Dehydration/rehydration; *In situ* HT-SCXRD; Channels distortion

1 Introduction

Armstrongite, $CaZr[Si_6O_{15}]\cdot 2H_2O$, is a natural "zeolite-like" Zr-silicate with a heteropolyhedral framework consisting of SiO_4 tetrahedra and ZrO_6 octahedra that form cavities occupied by Ca-exchangeable cations [1,2]. Zr-silicates are also included among the mixed Octahedral-Pentahedral-Tetrahedral (OPT) microporous framework silicates which were largely studied for gas separation and optical and magnetic applications [3].

For such materials it is recognized that the chemical and physical processes depend on the hydration degree of the extra-framework cations, especially in relation to temperature changes [e.g. Refs. [4,5]]. As a consequence, the mechanisms of T-induced dehydration, cation migration and the rearrangement of extra-framework species in porous materials have been investigated, mainly by *in situ* single crystal or powder X-ray diffraction [e.g. Refs. [6–10]].

The room temperature (RT) armstrongite crystal structure was described in detail elsewhere [2]. In brief, the armstrongite structure consists of silicate sheets showing four- and six-member tetrahedral rings alternating along [010] and four- and eight-member tetrahedral rings alternating along [100] (Fig. 1*a*). The silicate $[Si_6O_{15}]$ sheets are connected by vertices to ZrO_6 octahedra to give the $(ZrSi_6O_{15})^{2-}$ heterogeneous framework. The seven-fold coordinated $CaO_5(H_2O)_2$ polyhedra are connected by edges to ZrO_6 octahedra, to form columns running parallel to [010] (Fig. 1*b*).

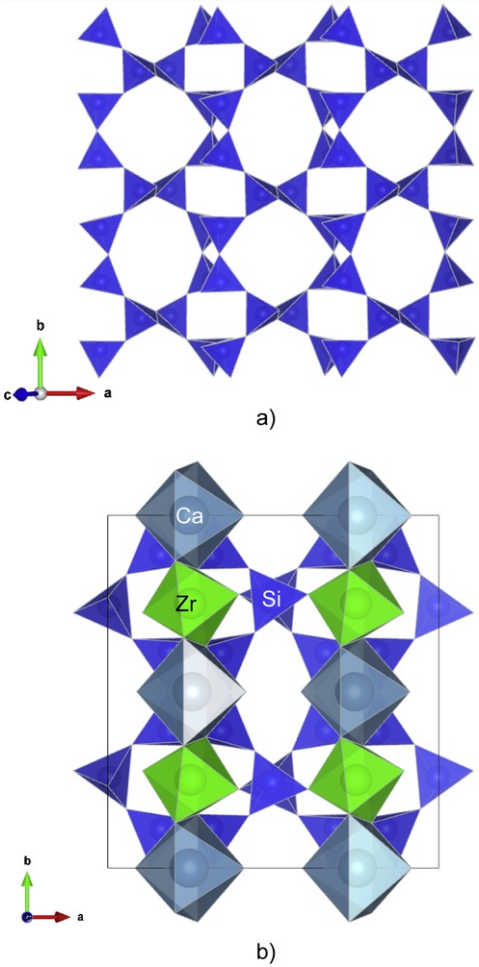

Fig. 1 Armstrongite silicate sheets showing four-, six-, and eight-member tetrahedral rings (*a*); armstrongite structure at RT seen along [001] (*b*). ZrO_6 octahedra, Ca-polyhedra, SiO_4 tetrahedra and oxygen atoms are drawn in green, light-blue, blue and red, respectively. (For interpretation of the references to color in this figure legend, the reader is referred to the Web version of this article.)

alt-text: Fig. 1

The temperature-induced dehydration of armstrongite has been very recently investigated by means of thermal analysis, *in situ* X-ray powder diffraction and Fourier Transform Infrared spectroscopy [11]. The authors found that at ambient humidity the process starts at ~380 °C and is completed within few tenths of degrees; rehydration of the sample occurs at T ~320 °C under the conditions of the diffraction experiment and at T ~280–300 °C during the FTIR analysis. From the latter investigation, the evolution of the intensity of the $^{H2O}\nu_3$ stretching and $^{H2O}\nu_3$ bending bands showed a sudden decrease on heating at T > ~370 °C and a drastic drop in the 390–420 °C range. Upon cooling, the mineral completely recovered its water content. The dehydration/rehydration was found out to be quick and reproducible.

In the present study we track the dehydration process of armstrongite by *in-situ* High Temperature Single Crystal X-ray Diffraction (HT SCXRD) in order to determine for the first time the crystal structure of the partially and fully dehydrated phase.

2 Experimental methods

Single crystals of armstrongite from Khan Bogdo, Mongolia (same specimen as used by ~~Mesto et al.~~ [2], $(Ca_{0.96}Ce_{0.01}Yb_{0.01})Zr_{0.99}Si_6O_{14.97}\bullet\ 2.02H_2O$) were selected by an optical microscope, glued on the tip of a glass fiber and

mounted on a goniometer head.

For the high temperature experiment, diffraction data were collected on a BRUKER APEX II diffractometer equipped with MoKα radiation (λ = 0.71073 Å) and a CCD area detector. In particular, the dehydration process of armstrongite was monitored *in situ* both in air and in dry N_2 atmosphere (RH = 0).

In the first case, the crystal was heated by means of a Bruker AXS FR 559 device. The X-ray data were collected in the T-range 25–500 °C: for T > 400 °C in step of 50 °C, whereas in the T-range 300–400 °C a step of 25 °C was used. The heating rate was 5 °C/min and the equilibration time of approx. 30 min was set before starting fast data collection (2.5 h, $2\theta_{max} = 70°$) in order to derive cell parameters. At T = 450 °C a complete data collection (9 h, $2\theta_{max} = 80°$) was performed.

In the second case, a homemade heating device, consisting of a temperature controlled hot-nitrogen blower (1.4 l/min), was used. The data were collected from RT to 375 °C in steps of 25 °C. Before starting a new data collection, the crystal was equilibrated for ~40 min. Each data collection lasted ~6 h.

In both the experiments, an inspection of the reciprocal space indicated, for each data set, the occurrence of two domains of reflections related by twinning. To estimate the correct unit cell, the reflections belonging to the two components were manually separated and indexed independently. Data integration (SAINT V8.27B [12]) was then performed by keeping a fixed box-size and fixed unit cell parameters. An empirical absorption correction was applied (SADABS, 2012). Structures refinements were carried out with SHELXL-2014 [13] using neutral atomic scattering factors and starting from atomic coordinates in ~~Mesto et al.~~ [2]. The relatively low quality of the diffraction data from the crystal heated in air at 450 °C (presence of broadened and weak peaks, occurrence of high residual electron density-peaks in the difference Fourier map) did not allow to obtain a reliable model of the dehydrated armstrongite structure. By contrast, for the data collected under dry conditions, from RT to 325 °C the structures were all refined in the monoclinic space group *C*2/*m* (the same space group as found in ~~Mesto et al.~~ [2]). However, structure refinement of the dehydrated phase was also performed in space groups *C*2 and *Cm* in order to check for symmetry lowering. In both cases the associated R(σ) was higher (R(σ) = 0.1065 and 0.1035 for *Cm* and *C*2 respectively) compared to the value found for *C*2/*m* (R(σ) = 0.0725). In addition, the structural model in *Cm* was similar to that obtained in *C*2/*m*, whereas the refinements in *C*2 were not satisfactory (higher *R*1, $I > 2\sigma(I) = 0.0970$ and higher residuals in difference Fourier map). Thus, although local symmetry reduction cannot be excluded, the dehydrated phase maintains on average the centrosymmetric space group *C*2/*m*.

A detailed description of the dehydrated armstrongite structure, obtained at 275 °C and provided here for the first time, is given in the results and discussion section below. As previously reported [2], armstrongite was found to be twinned with two individuals rotated along a two-fold axis parallel to [001] (twin law: −100 0–10 001). The twin was handled by generating a (Insert a blank between "a" and ".hkl", please).*hkl* file with HKLF 5 format by using Platon/TwinRotMat software [14]. The fractional twin volumes (BASF parameter) are reported in Table 1.

Table 1 Crystal data and refinement parameters of armstrongite at RT, 225 °C (RH ≈ 0), 250 °C (RH ≈ 0), 275 °C (RH ≈ 0) and of armstrongite structure dehydrated at 375 °C (RH ≈ 0) and exposed to humid conditions for 21 days.

alt-text: Table 1

Crystal data	RT	225 °C	250 °C	275 °C	300 °C	Rehydrated_21d
a (Å)	14.0135(7)	14.009(3)	13.997(3)	13.406(3)	13.401(3)	14.009(3)
b (Å)	14.1234(6)	14.169(3)	14.152(3)	13.752(3)	13.704(3)	14.120(3)
c (Å)	7.8388(4)	7.8376(16)	7.8261(16)	7.8113(16)	7.7791(16)	7.8561(16)
β ("β" not in italics, please) (°)	109.401(4)	109.37(3)	109.35(3)	110.22(3)	110.18(3)	109.47(3)
V (Å^3)	1463.35(13)	1467.7(6)	1462.6(6)	1351.3(5)	1340.9(5)	1465.1(6)
Z	4	4	4	4	4	4
Space Group	*C*2/*m*	*C*2/*m*	*C*2/*m*	*C*2/*m*	*C*2/*m*	*C*2/*m*
Refined Chemical formula	$CaZrSi_6O_{15} \cdot 3H_2O$	$CaZrSi_6O_{15} \cdot 1.95H_2O$	$CaZrSi_6O_{15} \cdot 1.77H_2O$	$CaZrSi_6O_{15}$	$CaZrSi_6O_{15}$	$CaZrSi_6O_{15} \cdot 3H_2O$
Crystal size (mm^3)	0.18 × 0.10 × 0.10	0.18 × 0.10 × 0.10	0.18 × 0.10 × 0.10	0.18 × 0.10 × 0.10	0.18 × 0.10 × 0.10	0.18 × 0.10 × 0.10
Intensity measurement						
Diffractometer	Bruker APEX II	Bruker APEX II	Bruker APEX II	Bruker APEX II SMART	Bruker APEX II SMART	Bruker APEX II SMART

	SMART	SMART	SMART			
X-ray radiation	Mo$K\alpha$ λ = 0.71073 Å	Mo$K\alpha$ λ = 0.71073 Å	Mo$K\alpha$ λ = 0.71073 Å	Mo$K\alpha$ λ = 0.71073 Å	Mo$K\alpha$ λ = 0.71073 Å	Mo$K\alpha$ λ = 0.71073 Å
X-ray power	50 KV, 30 mA	50 KV, 30 mA	50 KV, 30 mA	50 KV, 30 mA	50 KV, 30 mA	50 KV, 30 mA
Monochromator	Graphite	Graphite	Graphite	Graphite	Graphite	Graphite
Temperature (°C)	25	225	250	275	300	25
Time per frame (s)	10	10	10	10	10	10
Max. 2θ (°)	57.3	58.33	57.59	50.68	44.59	56.81
Index ranges	$-18 \le h \le 17$	$-19 \le h \le 19$	$-18 \le h \le 17$	$-16 \le h \le 15$	$-14 \le h \le 14$	$-18 \le h \le 17$
	$-18 \le k \le 19$	$-18 \le k \le 19$	$-18 \le k \le 19$	$-16 \le k \le 16$	$-14 \le k \le 14$	$-18 \le k \le 18$
	$-5 \le l \le 10$	$-5 \le l \le 10$	$-5 \le l \le 10$	$-5 \le l \le 9$	$-8 \le l \le 8$	$-5 \le l \le 10$
No. of measured reflections	7984	9737	9425	6881	5455	9179
No. of unique reflections	1938	2065	1974	1293	908	1897
No. of observed reflections I > 2σ (I)	1529	1560	1513	921	738	1313
Structure refinement						
No. of parameters used in the refinement	124	129	129	124	114	125
$R(\sigma)$	0.0464	0.0525	0.0526	0.0725	0.1046	0.0693
GooF	1.060	1.049	1.062	1.050	1.078	1.169
$R1$, $I > 2\sigma$ (I)	0.0463	0.0490	0.0487	0.0750	0.1154	0.0956
$R1$, all data	0.0646	0.0678	0.0679	0.1047	0.1489	0.1294
$wR2$ (on F^2)	0.1114	0.1292	0.1262	0.2000	0.2911	0.2299
$\Delta\rho_{min}$ ($e^-/Å^{-3}$) close to	−0.91 O7	−0.66 Si1	−0.65 Zr1A	−0.82 Zr1	−0.87 Ca1B	−2.12 O9
$\Delta\rho_{max}$ ($e^-/Å^{-3}$) close to	1.01 O8	1.51 Zr1A	1.17 Zr1	0.91 Zr1	1.13 Si1	2.59 Zr1
BASF	0.272(4)	0.271(4)	0.271(4)	0.228(8)	0.293(16)	0.707(3)

To monitor the armstrongite rehydration, the same crystal used for the temperature-dependent data collection under dry conditions was removed from the diffractometer and exposed to high humidity conditions in a close container with approximately 100 ml of deionized water. Diffraction data were collected after 21 days of exposure. Data collections and refinements parameters are reported in Table 1.

All structure drawings have been produced by VESTA software [15]. Cif files of the refined crystal structures are submitted as supplementary material together with details on structure analysis (Tables from S1 to S5).

3 Results and discussion

3.1 Variation of unit cell parameters with T

The comparison between the evolution of the unit cell parameters and resulting cell volume in air and in N_2 atmosphere is illustrated in Fig. 2(*a*, *b*). The two data sets clearly show an abrupt discontinuity in the trend of the *a* and *b* parameters and of the unit-cell volume at T = 275 °C in dry conditions and at T = 450 °C in air. This evidence is associated with the dehydration process of the armstrongite structure as previously described in a high temperature X-ray powder diffraction study [11]. Due to the thermal expansion of the structure under both experimental conditions, the dehydration is preceded by a slight increase of the cell volume (up to 200 °C and 325 °C in N_2 atmosphere and

in air, respectively, Fig. 2*b*). This effect is particularly pronounced along the *b*-axis, Fig. 2*a*. In addition, the dehydration involves a cell volume decrease of ~7.5% compared to that measured at RT. This value is compatible with the loss of the two structural H_2O molecules ~~(Schingaro et al.~~ [11]~~)~~. Overall the above results indicate that dehydration of armstrongite involves a first order transition.

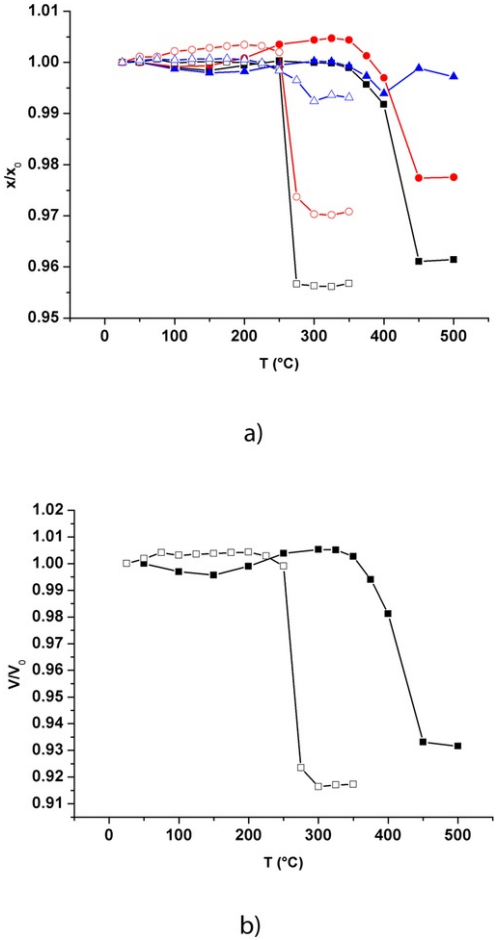

Fig. 2 Normalized unit cell parameters (*a*) and volume (*b*) of armstrongite *versus* temperature. Symbols: solid for the crystal heated in air; empty for the crystal heated in dry condition; a/a_0 (black squares); b/b_0 (red circles); c/c_0 (blue upward triangle). a_0, b_0, c_0 and V_0 are lattice parameters and unit cell volume at room temperature, respectively. (For interpretation of the references to color in this figure legend, the reader is referred to the Web version of this article.)

alt-text: Fig. 2

Note that the dehydration temperature in air was found to occur at 450 °C in the present work and in the T-range 375–400 °C for the XRPD experiment in ~~Schingaro et al.~~ [11]. Smaller crystal size and, therefore, shorter water path for the powder sample may explain the slightly lower value of the dehydration temperature found by ~~Schingaro et al.~~ [11]. Under dry conditions (RH = 0) the dehydration is shifted towards lower temperature.

Cell parameters acquired at room temperature after the rehydration process are very close to those obtained before the heating experiment (see Table 1).

3.2 The crystal structure of the dehydrated armstrongite

The armstrongite structure at RT was redetermined and the results agree with those of ~~Mesto et al.~~ [2]. The relevant data are deposited in Table S1. In summary, the RT armstrongite structure has *C*2/*m* symmetry with $a = 14.0135(7)$, $b = 14.1234(6)$, $c = 7.8388(4)$ Å, $\beta = 109.401(4)°$, $V = 1463.4(1)$ Å^3; the twin component ratio is 0.27/0.73 (Table 1). The calcium at Ca1 site is seven-fold coordinated by two H_2O molecules (oxygen atoms labeled W10 and

W11), and five framework oxygen atoms labeled O3 (× 2), O4 (× 2), and O5 (Fig. 3*a*, *c*).

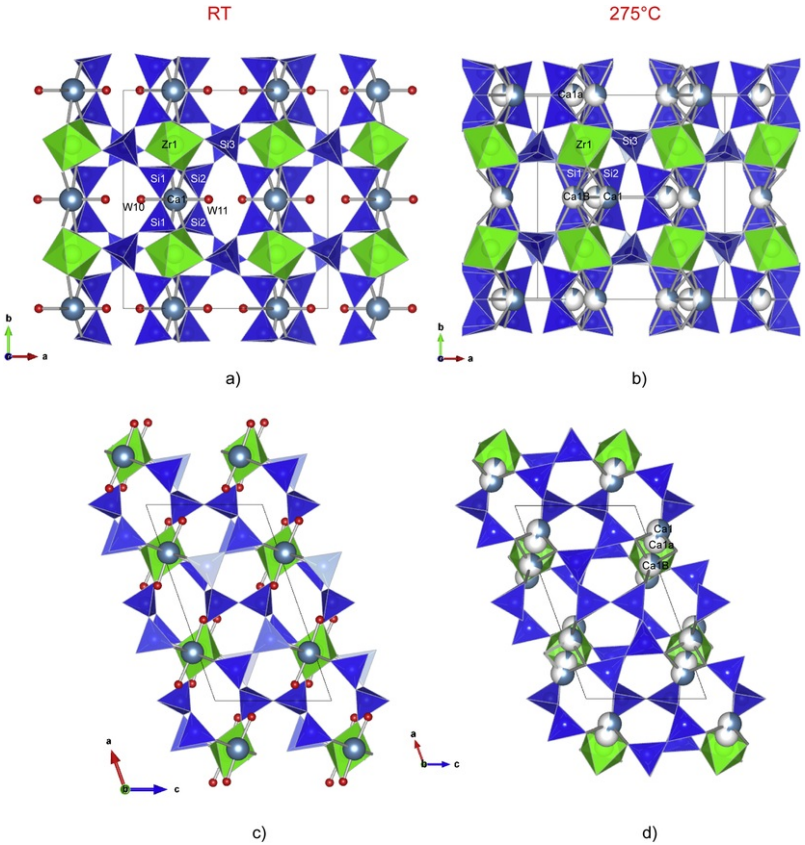

Fig. 3 Armstrongite structure at RT and at 275 °C projected along **c** (*a*, *b*) and **b** (*c*, *d*) axis. Colors as reported in Fig. 1. (*b*, *d*) Splitting of Ca atoms on three partially occupied sites: the occupancy of the three sites, Ca1, Ca1A and, Ca1B is indicated by partial colored spheres (*b*, *d*). (For interpretation of the references to color in this figure legend, the reader is referred to the Web version of this article.)

alt-text: Fig. 3

The dehydrated phase (at 275 °C) exhibits the same space group as RT armstrongite, significantly shortened *a* and *b* cell dimensions, increased β angle, and smaller unit-cell volume ($a = 13.406$ ~~(3)~~ (Round brackets include standard deviation. The correct typing is 13.406(3).), $b = 13.752(3)$, $c = 7.811(2)$ Å, $\beta = 110.22(3)°$, $V = 1351.3(5)$ Å^3) with respect to the hydrated phase (Table 1). The results of the full matrix anisotropic structure refinement are shown in Tables 2 and 3, whereas in Fig. 3*b*, *d* the structural features of dehydrated armstrongite are illustrated. The heteropolyhedral framework is more distorted than in the RT structure. The Ca1 RT site splits into three positions (Ca1, Ca1A and Ca1B); splitting of framework oxygen sites was also observed (see Table 2 and below). After the loss of the H_2O molecules the bond distance increased from 2.43(2) to 2.58(1) Å (Table 3). The details of the transformation from RT to the dehydrated phase are reported in the following paragraph.

Table 2 Atomic coordinates, U_{eq} (Å^2), and occupancies of armstrongite structure at 275 °C (RH ≈ 0) and of armstrongite structure dehydrated at 375 °C (RH ≈ 0) and exposed to humid conditions for 21 days.

alt-text: Table 2

275 °C						
Site	Scattering Factor	*x*	*y*	*z*	U_{eq}	*Occ. (Delete the border (bold line) below this row. It is unnecessary)*

Ca1	Ca	0.3698(8)	0.5	0.1186(11)	0.074(3)	0.580(11)§
Ca1A	Ca	0.313(3)	0.5	0.060(4)	0.029(7)	0.1§§
Ca1B	Ca	0.1923(12)	0.5	−0.0521(19)	0.081(5)	0.320(11)§
Zr1	Zr	0.25	0.25	0	0.0567(6)	1
Si1	Si	0.2096(3)	0.61130(19)	0.3378(4)	0.0502(8)	1
Si2	Si	0.3675(2)	0.61130(19)	0.7429(4)	0.0460(8)	1
Si3	Si	0.0008(3)	0.7229(3)	0.2988(4)	0.0603(9)	1
O1	O	0	0.7212(8)	0.5	0.078(4)	1
O2	O	0.2784(7)	0.6236(6)	0.5467(10)	0.070(2)	1
O3	O	0.3238(7)	0.6369(7)	0.9003(11)	0.074(2)	1
O4	O	0.2653(7)	0.6494(9)	0.2060(12)	0.098(3)	1
O5	O	0.2314(17)	0.5	0.276(3)	0.061(4)	0.517(15)*
O5A	O	0.1576(19)	0.5	0.313(3)	0.061(4)	0.483(15)*
O6	O	0.378(3)	0.5	0.789(3)	0.050(4)	0.43(2)**
O6A	O	0.4286(19)	0.5	0.773(3)	0.050(4)	0.57(2)**
O7	O	0.4724(7)	0.6668(7)	0.7475(14)	0.091(3)	1
O8	O	0.096(3)	0.6803(16)	0.288(6)	0.067(5)	0.483(15)*
O8A	O	0.097(3)	0.6350(15)	0.297(5)	0.067(5)	0.517(15)*
O9	O	−0.1094(13)	0.7050(15)	0.154(2)	0.061(3)	0.57(2)**
O9A	O	−0.1017(17)	0.667(2)	0.151(3)	0.061(3)	0.43(2)**
Rehydrated_21 d						
Site	Scattering Factor	*x*	*y*	*z*	U_{eq}	*Occ.*
Ca1	Ca	0.2544(3)	0.5	0.0489(5)	0.0309(9)	1
Zr1	Zr	0.25	0.25	0	0.0203(10)	1
Si1	Si	0.1869(3)	0.6142(2)	0.3395(5)	0.0250(8)	1
Si2	Si	0.3415(3)	0.6105(2)	0.7313(5)	0.0245(8)	1
Si3	Si	0.0031(2)	0.7418(3)	0.3022(4)	0.0242(7)	1
O1	O	0	0.7679(8)	0.5	0.036(3)	1
O2	O	0.2587(8)	0.6402(6)	0.5398(12)	0.036(2)	1
O3	O	0.2974(7)	0.6278(6)	0.8904(13)	0.029(2)	1
O4	O	0.2284(8)	0.6537(6)	0.1856(13)	0.032(2)	1
O5	O	0.1816(11)	0.5	0.3074(19)	0.032(3)	1
O6	O	0.3731(11)	0.5	0.727(2)	0.034(3)	1
O7	O	0.4449(7)	0.6684(6)	0.7584(13)	0.032(2)	1

O8	O	0.0740(8)	0.6494(6)	0.3139(15)	0.038(3)	1
O9	O	−0.1052(7)	0.7234(6)	0.1619(13)	0.034(2)	1
W10	O	0.0873(14)	0.5	−0.146(3)	0.065(6)	1
W11	O	0.4183(15)	0.5	0.267(3)	0.070(6)	1

§ *Occ.* Ca1 = 1-*Occ.* Ca1B.

§§ *Occ.* Ca1A = fixed to 1- *Occ.* (Ca1 + Ca1B).

* *Occ.* O5= *Occ.*O8A = 1-*Occ.*O5A = 1-*Occ.*O8.

** *Occ.* O6 = *Occ.*O9A = 1-*Occ.*O6A = 1-*Occ.*O9.

Table 3 Bond distances of armstrongite structure at 275 °C (RH ≈ 0) and of armstrongite structure dehydrated at 375 °C (RH ≈ 0) and exposed to humid conditions for 21 days. Non-occurring distances are reported in italics.

alt-text: Table 3

275 °C (Delete the border (bold line) below this row. It is unnecessary)			
Zr1-O9 × 2	1.953(17)	Si3-O9	1.539(16)
Zr1-O4 × 2	2.077(9)	Si3-O1	1.575(3)
Zr1-O3 × 2	2.130(8)	Si3-O7	1.629(10)
Zr1-O9A × 2	2.24(2)	Si3-O8	1.43(4)
		Si3-O9A	1.65(2)
		Si3-O8A	1.77(3)
Si1-O8A	1.47(3)		1.60
Si1-O4	1.558(9)		
Si1-O2	1.581(8)	Ca1-Ca1A	*0.74(3)*
Si1-O8	1.72(3)	Ca1-W10	*2.290(19)*
Si1-O5	1.660(9)	Ca1-O3 × 2	2.471(10)
Si1-O5A	1.665(10)	Ca1-O6A	2.54(3)
	1.61	Ca1-O6	2.62(3)
		Ca1-O5	2.56(2)
Si2-O3	1.574(8)	Ca1-O4 × 2	2.703(12)
Si2-O7	1.589(9)		2.58(1)
Si2-O2	1.593(8)		
Si2-O6	1.567(6)	Ca1B-O9A × 2	2.58(3)
Si2-O6A	1.71(11)	Ca1B-O3 × 2	2.691(14)

	1.61	Ca1B-O4	2.807(15)
O5-O5A	*1.12(3)*	Ca1A-O3 x2	2.291(18)
O6-O6A	*0.73(2)*	Ca1A-O5	2.31(4)
O8-O8A	*0.63(3)*	Ca1A-O4 x2	2.54(2)
O9-O9A	*0.54(3)*	Ca1A-O6	2.55(4)
Rehydrated			
Zr1-O9 × 2	2.038(9)	Si3-O9	1.572(10)
Zr1-O4 × 2	2.088(9)	Si3-O1	1.612(4)
Zr1-O3 × 2	2.131(9)	Si3-O7	1.612(9)
		Si3-O8	1.623(10)
Si1-O4	1.607(10)		1.60
Si1-O2	1.602(10)		
Si1-O8	1.605(11)	Ca1-W10	2.332(18)
Si1-O5	1.630(4)	Ca1-W11	2.36(2)
	1.61	Ca1-O3 × 2	2.380(9)
		Ca1-O4 × 2	2.502(9)
Si2-O3	1.587(10)	Ca1-O5	2.558~~[14]~~ (Change the square brackets with round brackets, please: the correct value is 2.558(14))
Si2-O7	1.614(10)		
Si2-O2	1.619(10)		
Si2-O6	1.626(5)		
	1.61		

3.3 Structural modifications upon heating

With increasing temperature, the armstrongite structure did not change significantly up to 200 °C whereas at 225 °C the mineral started releasing water at W11 site (occ. = 0.95(2)). Simultaneously, the H_2O located at W10 displayed positional disorder and was split in two positions, W10 and W10A, 0.61(2) Å apart (Table S2). Residual electron density (>1.5 $e^-/Å^3$) was also detected at ~ 0.5 Å from the Zr1 site and modeled by splitting the Zr atom over two positions at Zr1 and Zr1A sites (Table S2). As the dehydration proceeded, additional water was lost at 250 °C from W11 (occ. = 0.77(2)) (Table S3). At 275 °C, the unit-cell volume significantly dropped to 1351.3(5) $Å^3$ (Table 1, Fig. 2*b*) accompanied by a distortion of the framework (Fig. 3*b*, *d*). At this temperature the W11 was empty. The structure was assumed to be anhydrous although electron density (6 $e^-/Å^3$) was detected at the W10 site. The latter density, was refined with the Ca scattering factors (Table 2). This interpretation was suggested by the following features: i) the occupancy of the Ca1 site decreased to ~0.6; ii) the occupancy of the W10 site converged to ~0.3; iii) the occurrence of a new low occupied site at ~0.7 Å from Ca1 (Ca1A) led to a total occupancy Ca1 + W10 (renamed Ca1B) + Ca1A = 0.96(6), without any constraints on the refined occupancies. Thus, the final structural model with Ca splitting into three subsites Ca1, Ca1B and Ca1A without residual H_2O at W10, was adopted (Table 2). In addition, the framework oxygen sites at O5, O6, O8 and O9 showed positional disorder and were split over O5A, O6A, O8A and O9A, respectively

(Table 2). Subsequent increase of temperature to 300 °C did not cause significant structural modifications but the reflections became significantly smeared and their intensities weakened increasing the R index (Table 1, Table S4). At 325 and 350 °C only cell parameters were extracted.

The dehydrated structure at 275 °C is characterized by a contraction of the unit cell (Table 1) and the eight-membered ring channels became more elliptical (Fig. 3*b*, *d*) than in the RT structure (Fig. 3*a*, *c*). This contraction is due to the Ca migration along [$\bar{1}01$] as a consequence of the water loss. With increasing temperature, the Ca1 site starts approaching the W10 position (Fig. 4). However, when the structure becomes anhydrous, at 275 °C, Ca disorderly distributes over different sites: Ca1 and Ca1A roughly approach the previous W11 site; the Ca1B subsite is intermediate (*0.19,½,-0.05*) between the original Ca1 site and the position previously occupied by the H_2O molecule at W10. The splitting of Ca atoms over the Ca1, Ca1A, and Ca1B sites is necessary to maintain a favorable coordination in absence of H_2O. At 275 °C, the Ca1 site is still seven-fold coordinated (Table 3) whereas the Ca1B forms bonds with 5 oxygen (two at O9A, two at O3 and one at O4 site) plus two longer ones with O9 site.

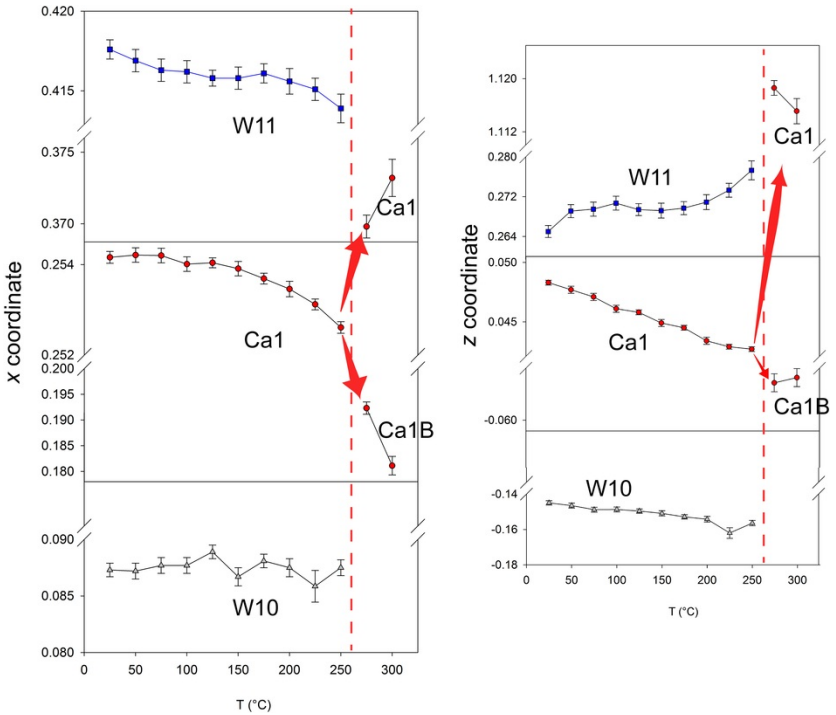

Fig. 4 Trend of atomic coordinates (*x* and *z*) of Ca1, W10 and W11 sites with increasing temperature. At 275 °C and 300 °C the W10 site is assumed to be occupied by Ca atoms. The red arrows indicate the migration of the original Ca site toward the positions occupied by H_2O at W10 and W11 in the hydrated structure. (For interpretation of the references to color in this figure legend, the reader is referred to the Web version of this article.)

alt-text: Fig. 4

The Ca migration is accompanied by the tilting of the Zr octahedra and of the Si tetrahedra as a response to the pulling effect of Ca on the framework oxygen (see Fig. 5). At RT, and up to 225 °C, the Ca is seven-fold coordinated by the two H_2O at W10 and W11, four framework oxygen sites 2 × O3 and 2 × O4, shared between Zr1 and Si2 and Zr1 and Si1 respectively, and by the one at O5, which is the oxygen bridge between the two Si1 sites (see Fig. 5). Such configuration, as well as the framework arrangement, does not change until the transformation to the anhydrous phase occurs. When the structure dehydrates, new bonds to O6 and O6A (from Ca1) and to O9A (from Ca1B) form (Fig. 5). The formation of these new Ca-O links results in a change of the shape of the eight-membered rings, referred as I and II in Fig. 5, which become more elliptical than those of the RT framework. If O-O contacts in channel I are considered, the O5-O6 distance increases from 7.653(10) at RT to 7.835(4) Å at 275 °C whereas the O9-O9 distance decreases from 6.319(6) to 5.12(3) Å, respectively. The same distances shorten and lengthen correspondingly in channel II. The distortion of the eight-membered rings is also accompanied by a modification of the other tetrahedral rings (six- and four-membered) parallel to (101) (Fig. 6). As a consequence, the entire silicate sheet of the dehydrated structure is more corrugated ($\Delta z_{[100]} = 0.381$ and $\Delta z_{[010]} = 0.779$ at T = 275 °C**)** with respect to that of the hydrated phase ($\Delta z_{[100]} = 0.173$ and $\Delta z_{[010]} = 0.569$ at T = 25 °C**)**. Such corrugation, which corresponds to a deviation from coplanarity of the unshared O atoms on the $(1\,1\,\bar{1})$ plane, is required in order to bring the O atoms sufficiently close to the Zr cations.

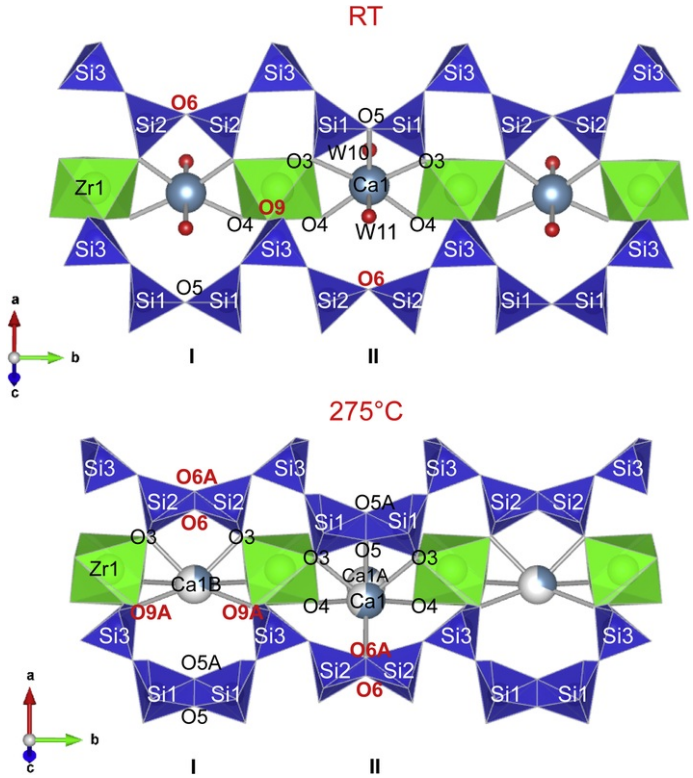

Fig. 5 Channels I and II in armstrongite structure at RT and at 275 °C. Colors as reported in Fig. 1. (For interpretation of the references to color in this figure legend, the reader is referred to the Web version of this article.)

alt-text: Fig. 5

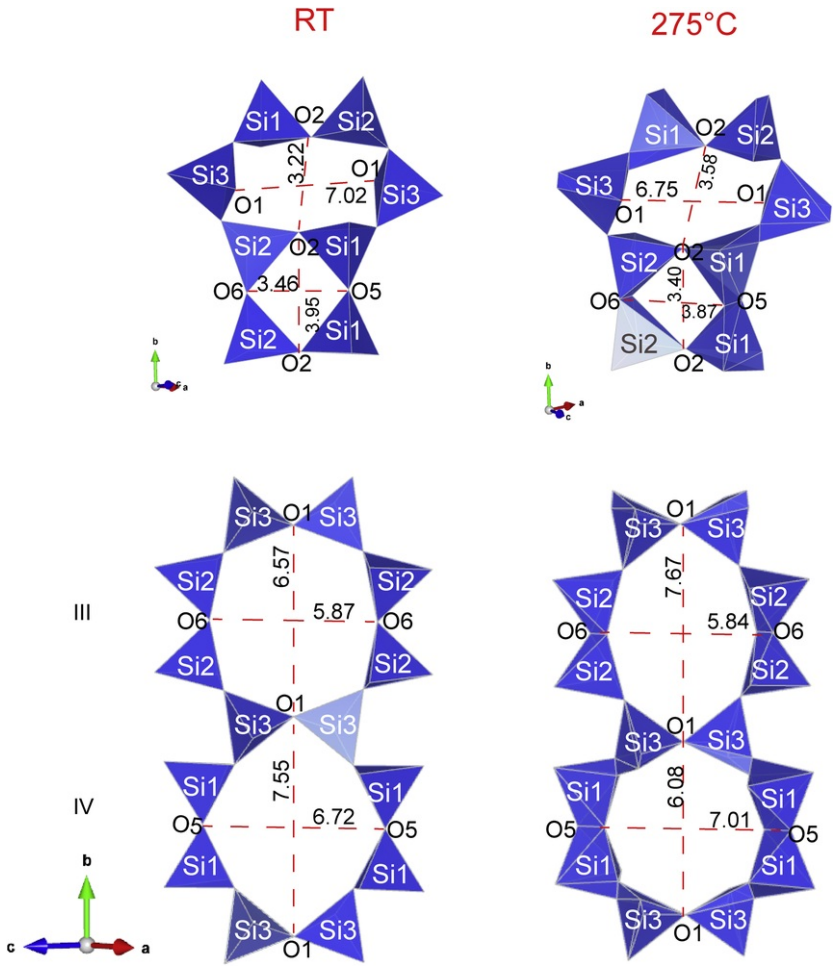

Fig. 6 Two channels, referred as III and IV, constituted only by SiO_4 tetrahedra, in armstrongite structure at RT and at 275 °C. The O-O distance between of the shortest and longest diagonal [16] is reported in Å.

alt-text: Fig. 6

3.4 Rehydration and comparison with elpidite

The crystal structure of the rehydrated armstrongite obtained after 21 days exposure to humid conditions indicated that the mineral was able to recover all the structural water. Indeed, the unit-cell volume was similar to that measured at RT (Table 1). Nevertheless, the structural refinement indicated several residual peaks in difference Fourier maps. The highest peak (2.21 $e^-/Å^3$) resulted at 0.80 Å from the W10 site whereas peaks with density between 1.1 and 1.8 $e^-/Å^3$ were mainly detected close to the framework oxygen and Ca1 sites. An attempt to insert these peaks in the final structural refinement was not successful. According to the positions of the residual peaks, they can be interpreted as relicts of the structural modification of the dehydrated structure. Similar to the partially hydrated structure, positional disorder was found to affect the Zr octahedron and such disorder was initially modeled by inserting an additional Zr site. However, the refinement provided low occupancy (0.024(7)) for this additional site and eventually it was not inserted in the final model (Tables 2 and 3).

The rehydration behavior of the armstrongite single crystal confirms that the dehydration/rehydration process of this mineral is completely reversible as previously noticed by Schingaro et al. [11]. The complete recovery of water and corresponding transformation back to the RT modification is surprising if the armstrongite behavior is compared with that of elpidite [10]. The latter, once dehydrated, after 30 days immersion in water, could recover only 10% of the original H_2O content and, most significantly, the structure preserved the contracted unit-cell volume (−3.4% compared to that measured at RT) of the dehydrated phase [10]. Such behavior was attributed to the narrowing of

the main structural windows (the eight-membered ring channels constituted by SiO_4 and ZrO_6 polyhedra) which hindered the water reabsorption.

In armstrongite the eight-membered ring channels, which are equivalent to those of elpidite (Fig. 5), also shrink as a consequence of dehydration. However, differently from elpidite, two additional eight-membered ring apertures (referred as channel III and channel IV) are accessible to extra-framework occupants: one is formed by four Si3 and four Si1 tetrahedra and the other one by four Si2 and four Si3 tetrahedra (Fig. 6). In Table 4 the size of channel apertures of armstrongite measured at RT and at 275 °C, respectively, are reported. Note that the channels III and IV almost maintain the original elliptical shape whereas the channels I and II mostly vary their shape by increasing the L/S ratio from 1.21 at RT to 1.53 at 275 °C. In elpidite the compression of the channels is much more pronounced with values of L/S ratio increasing from 1.05 at RT to 1.60 and 1.42 at 250 °C (in the anhydrous structure there are two symmetry distinct eight-membered ring channels). Thus, in contrast to elpidite, in armstrongite the water can easily access the structural voids and be reabsorbed.

Table 4 L/S ratio of the longest and shortest diagonals [16] of eight-membered ring channels in armstrongite at RT and at 275 °C shown in Figs. 5 and 6.

alt-text: Table 4

	Sites forming the channel	O-O distance	RT	275 °C
Channel I, II	2 Si1, 2 Si2, 2 Si3, 2 Zr1	O5-O6	7.653(10)	7.835(4)
		O9-O9	6.319(6)	5.12(3)
		L/S	1.21	1.53
Channel III	4 Si2, 4 Si3	O1-O1	6.570(8)	7.668(16)
		O6-O6	5.866(7)	5.835(4)[a]
		L/S	1.12	1.31
Channel IV	4 Si1, 4 Si3	O1-O1	7.553(8)	6.084(16)
		O5-O5	6.720(7)	7.01(3)[b]
		L/S	1.12	1.15

[a] mean value between O6-O6 and O6A-O6A.

[b] mean value between O5-O5 and O5A-O5A.

4 Conclusions

The high temperature study of armstrongite single crystal evidences that the mineral dehydrates at 450 °C in air and at 275 °C in N_2 atmosphere. The structure evolution with increasing temperature entails: 1) same space group (*C*2/*m*) with respect to the RT phase; 2) volume contraction compatible with the loss of both structural water molecules; 3) gradual migration of Ca cations resulting in splitting of the original Ca1 site to Ca1, Ca1A, Ca1B; 4) positional disorder of the O5, O6, O8 and O9 framework oxygen atoms; 5) tilting of Zr octahedra and Si tetrahedra, 6) channels distortion as well as modification of L/S ratio of the heteropolyhedral- and tetrahedral-rings with respect to the RT phase. Finally, the rehydrated armstrongite completely recovers the structural water. Thus, the dehydration/rehydration process is completely reversible, indicating that this Zr-silicate, differently from its Na-analogue, elpidite, truly behaves as a zeolitic material.

Conflicts of interest

There are no conflicts to declare.

Acknowledgments

The manuscript benefited from the useful comments by Thomas Armbruster and two anonymous referees.

Appendix A. Supplementary data

Supplementary data related to this article can be found at https://doi.org/10.1016/j.micromeso.2018.08.008.

Uncited references

[12]; [17].

References

[1] N.V. Chukanov, A.I. Kazakov, V.V. Nedelko, I.V. Pekov, N.V. Zubkova, D.A. Ksenofontov, Y.K. Kabalov, A.A. Grigorieva and D. Yu, Pushcharovsky, In: S.V. Krivovichev, (Ed), *Minerals as Advanced Materials II,* 2012, Springer, 167–179.

[2] E. Mesto, E. Kaneva, E. Schingaro, N. Vladykin, M. Lacalamita and F. Scordari, *Am. Mineral.* **99**, 2014, 2424–2432.

[3] J. Rocha and Z. Lin, In: G. Ferraris and S. Merlino, (Eds.), *Reviews in Mineralogy and Geochemistry* **vol. 57**, 2005, Mineralogical Society of America; Washington, 173–201.

[4] Y. Kuwahara, D. Kang, J.R. Copeland, N.A. Brunelli, S.A. Didas, P. Bollini, C. Sievers, T. Kamegawa, H. Yamashita and C.W. Jones, *J. Am. Chem. Soc.* **134**, 2012, 10757–10760.

[5] F.M. Higgins, H. De Leeuw and S.C. Parker, *J. Mater. Chem.* **12**, 2002, 124–131.

[6] D.L. Bish and J.W. Carey, In: D.L. Bish and D.W. Ming, (Eds.), *Reviews in Mineralogy and Geochemistry* **vol. 45**, 2001, Mineralogical Society of America; Washington, 403–452.

[7] G. Cruciani, *J. Phys. Chem. Solid.* **67**, 2006, 1973-1194.

[8] S.H. Park, J.B. Parise, M.E. Franke, T. Seydel and C. Paulmann, *Microporous Mesoporous Mater.* **108**, 2008, 1–12.

[9] R.M. Danisi, T. Armbruster and B. Lazic, *J. Solid State Chem.* **197**, 2013, 508–516.

[10] G. Cametti, T. Armbruster and M. Nagashima, *Microporous Mesoporous Mater.* **227**, 2016, 81–87.

[11] E. Schingaro, M. Lacalamita, E. Mesto and G. Della Ventura, *Microporous Mesoporous Mater.* **272**, 2018, 137–142.

[12] Bruker (2007) Bruker AXS Inc., Madison, Wisconsin, USA.

[13] G.M. Sheldrick, *Acta Crystallogr.* **C71**, 2015, 3–8.

[14] A.L. Speck, *J. Appl. Crystallogr.* **36**, 2003, 7–13.

[15] K. Momma and F. Izumi, *J. Appl. Crystallogr.* **44**, 2011, 1272–1276.

[16] T. Bauer and W.H. Baur, *Eur. J. Mineral* **10** (1), 1998, 133–147.

[17] N.E. Breese and M. O'Keeffe, *Acta Crystallogr.* **B47**, 1991, 192–197.

Appendix A. Supplementary data

The following are the supplementary data related to this article:

Multimedia Component 1

MICMAT-D-18-01025

alt-text: MICMAT-D-18-01025

Multimedia Component 2

armstr_RT.cif

alt-text: armstr_RT.cif

Multimedia Component 3

armstr275.cif

alt-text: armstr275.cif

Multimedia Component 4

armstr_rehy_21d.cif

alt-text: armstr_rehy_21d.cif

Graphical abstract

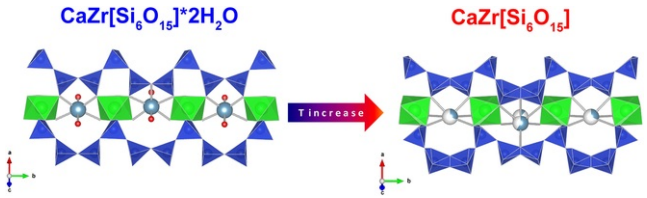

alt-text: Image 1

Highlights

- The dehydration of armstrongite, a zeolite-like mineral, was studied.
- The mineral dehydrates at 450 °C in air and at 275° in N_2 atmosphere.
- The process involves a phase transition without symmetry change.
- The dehydrated structure is disordered and distorted with respect to the hydrated one.
- The mineral, differently from similar compounds, truly behaves as a zeolitic material.

Queries and Answers

Query: Please confirm that the provided email “emanuela.schingaro@uniba.it” is the correct address for official communication, else provide an alternate e-mail address to replace the existing one, because private e-mail addresses should not be used in articles as the address for communication.
Answer: "emanuela.schingaro@uniba.it" is the correct address for official communication but it is misplaced. It should be inserted after E. Schingaro because E.Schingaro is the corresponding author

Query: Please note that author’s telephone/fax numbers are not published in Journal articles due to the fact that articles are available online and in print for many years, whereas telephone/fax numbers are changeable and therefore not reliable in the long term.
Answer: OK

Query: Correctly acknowledging the primary funders and grant IDs of your research is important to ensure compliance with funder policies. We could not find any acknowledgement of funding sources in your text. Is this correct?

Answer: Yes

Query: Uncited references: This section comprises references that occur in the reference list but not in the body of the text. Please position each reference in the text or, alternatively, delete it. Any reference not dealt with will be retained in this section. Thank you.
Answer: Actually, reference [12] is cited in the "Experimental methods" section. Reference [17] is cited in supplementary data file

Query: Please confirm that given names and surnames have been identified correctly and are presented in the desired order and please carefully verify the spelling of all authors' names.
Answer: Names, surnames and order are OK, but M.Lacalamita **is not** the corresponding author. The corresponding author is **E.Schingaro**

Query: Your article is registered as a regular item and is being processed for inclusion in a regular issue of the journal. If this is NOT correct and your article belongs to a Special Issue/Collection please contact e.bennitta@elsevier.com immediately prior to returning your corrections.
Answer: Yes